SIZE MEASUREMENTS OF FLUORESCENT CARBON NANOPARTICLES IN A CO-FLOWING LAMINAR DIFFUSION FLAME BY TIME-RESOLVED FLUORESCENCE ANISOTROPY

P. Minutolo*, M. Commodo, C. de Lisio***, A. D'Anna****
mario.commodo@unina.it
* Istituto di Ricerche sulla Combustione, CNR, P.le Tecchio, 80, 80126, Napoli, Italy
** Dipartimento di Ingegneria Chimica, Università di Napoli "Federico II", P.le Tecchio, 80, 80126, Napoli, Italy
***Centro di Ricerca e Sviluppo "Coherentia," C.N.R.–I.N.F.M., Unità di Ricerca di Napoli, and Dipartimento di Scienze Fisiche, Università di Napoli "Federico II," Complesso di Monte S. Angelo, Via Cintia, 80126, Napoli, Italy

Abstract
The mean size of flame-formed fluorescent carbonaceous nanoparticles was detected by in-situ time-resolved fluorescence anisotropy (TRFA) measurements. A well-known and long investigated co-flowing laminar diffusion flame of ethylene was used as combustion system for both data comparison and for its importance in the field of particulate formation and emission control. Form the analysis of the decay time of the fluorescence anisotropy, we estimated the diameter of particles selected by their ability to absorb and emit visible light, as function of the flame radius for several heights form the fuel nozzle. TRFA has allowed to investigate intermediate class of compounds between the UV absorbing particles and soot studied in previous works. These compounds have average sizes ranging from 5 to 15 nm. The technique proves to be applicable to the study of soot formation mechanisms, and specifically to follow the inception phenomena based on the transition from the gas-phase to the solid particles.

Introduction

The processes leading to the formation of particulate matter from the combustion of gas and liquid-phase fossil fuels and biomass is an active field of research because of their adverse effects on human health and on the environment. Combustion-formed particles range from very large aggregates in the micrometer-size range down to fine and ultrafine particles in the nanometer-size range [1]. The largest particles mainly have inorganic nature and can be successfully removed from combustion exhausts in suitable gas-cleaning devices. A relevant number of the particles formed at high-temperature, in the gas-to-particle transitions regions are of nanometric size, molecular-like nature and difficult to intercept in the gas-cleaning devices and thus contributing to air pollution. They are often referred to as nanoparticles or ultrafine particles. The emission of these particles in the atmosphere constitutes a serious concern for our health and for their contribution to photochemical smog. The smallest, organic particles play a particularly important role in health since they dominate size distributions in terms of number concentration and they are able to penetrate deeper than larger particles into the respiratory system [2, 3]. They could also affect the radiation balance of the atmosphere by serving as condensation nuclei for the formation of clouds and of contrails in the upper atmosphere [4]. Such combustion-generated nanoparticles have a peculiar chemical composition and morphology since they maintain molecular characteristics in terms of chemical reactivity, but at the same time exhibit transport and surface related phenomena typical of particles. Many new diagnostic tools, which allow analysis on an almost atomic level have been developed, or borrowed from molecule-based natural sciences. Their use improves our knowledge about the physical and chemical properties of combustion-formed nanoparticles and also about the kinetics of particle formation in combustion environments [1]. One technique very promising for in-situ characterization of organic particle in combustion environment is Time Resolved Fluorescence Anisotropy (TRFA) since this method allows determining the average size of classes of particles selected on the base of their spectroscopic properties. This is achieved by monitoring the rotational motion of photo-selected particles. The analysis of time decay of fluorescence anisotropy gives the size of those particles that can absorb the excitation beam and emit fluorescence, so that it allow gathering information on chemical and physical properties of the particles. TRFA is usually employed for studying biological molecules in liquid solvents [5]. It was applied for the first time in combustion for the measurement of NOC particles sampled from a premixed flame and suspended in water [6-8]. Only few works have extended this method to molecules in the gas phase [9,10]. In gas phase environment, friction forces strongly reduce so that hydrodynamic theory cannot be used and particle motion has to be described by collisional theories. The motion develops on a sub-nanosecond time scale and it is further made more complex by partial persistence of coherence. The applicability of TRFA to particles in flames was demonstrated in a previous work done in a propane Bunsen-type flame by the use of an ultra-short laser excitation and a streak-camera as detector to achieve the required time resolution [11]. In the present work, we use this technique to study particles in a co-flowing laminar diffusion flame similar to that one studied by Santoro and co-workers [12, 13]. This is a well-know and characterized flame, which may be used to verify the capability of our proposed method. Such a flame, in fact, has been subject of numerous numerical and experimental investigations in the last two decades. [12-22]. Conversely, the in situ determination of sizes of molecular-particles, selected on the bases of their spectroscopic properties, will add relevant information to complete the picture of particle formation in diffusion flames. It is still relevant to note that TRFA method, which is based on point measurements, is not affected by the uncertainties of inversion procedure as the line of sight light absorption, which limit the accuracy of volume fraction and sizes determined by lightabsorption/scattering method in this flame.

Theoretical section

The time evolution of fluorescence anisotropy is an important tool to obtain information on the dynamics of photo-selected molecules in a medium. Rotational and diffusional motions are determined by collision between solute and bath molecules, in particular by the rate of collisions and by the effectiveness of collisions in transferring angular momentum. At high density, the dynamics is determined by collective response of the medium and is described by the continuum approximation while at low density it is determined mainly by binary collisions. Which of the two regimes is able to describe particle dynamic depends on the time scale of interaction between fluorescent molecules and medium molecules, in particular duration of collision, time between two collisions and coherence time for orientational motion. Various models have been developed to describe the dynamic of a molecule in a medium.

The Langevin model describe the force acting on the molecule as composed by two terms, a frictional force which is proportional to the angular velocity ω and a random torque F [9-10]. This hypothesis is strictly valid for the motion of a slow heavy particle in a medium of light molecules, and the momentum transfer is proportional to the velocity of the heavy molecule

$$I\frac{\partial\omega(t)}{\partial t} = -\xi I\omega(t) + F \tag{1}$$

Where I is the moment of inertia of the molecule, ξ is the reduced friction coefficient and the standard friction coefficient is $\zeta=\xi I$. Other assumptions are at the bases of this theory. One is that the average value of random torque is zero; there is a low correlation time for the random force, which is expected to be not correct at high density where collective response of the medium can happen; and there is no correlation between initial velocity and random torque.

In this model, the angular velocity autocorrelation has an exponential decay with a decay time $\tau_\omega=1/\xi$, which differs on the molecular collision time according to how effective are collisions in changing the angular momentum of the molecule.

One quantity, which allows monitoring the microscopic dynamics, is the macroscopic polarization anisotropy. This experimental quantity is defined as

$$r(t) = \frac{I_{//} - I_{\perp}}{I_{//} + 2I_{\perp}} \tag{3}$$

Where $I_{//}$ and $I_{\perp}$ are the components of fluorescence intensity with polarization parallel and orthogonal to that of excitation beam. This quantity records the average orientation of transition dipole moments of photo-selected molecules with respect to the excitation dipole.

The analytical expression for transient anisotropy, which is valid in the limit of small angular steps, is the following:

$$r(t) = 0.4\exp\left\{\frac{-6KT}{I}\left(\tau_\omega{}^2 e^{-t/\tau_\omega} + t\tau_\omega - \tau_\omega{}^2\right)\right\} \tag{4}$$

For $t>>\tau_\omega$

The anisotropy decays exponentially:

$$r(t) \propto \exp\left(\frac{-6KT\tau_\omega}{I}t\right) \tag{5}$$

and gives the diffusive limit with exponential decay rate equal to $\tau_{rot}=1/(6D_r)$ and $D_r=KT/(\xi I)=KT\tau_\omega/I$

For $t<<\tau$, The molecules behave as free rotator and the expression of anisotropy:

$$r(t) = 0.4\exp\left(\frac{-3KT}{I}t^2\right) \tag{6}$$

describes the early time limit of free inertial motion. In this regime, the anisotropy is not influenced by the medium so that it is independent on ξ and the decay of anisotropy is Gaussian. The width of the curve depends on the size of the molecule through the moment of inertia.
The reduced coefficient of rotational friction can be obtained from hydrodynamic theories of transport phenomena in a medium. The theory of Chapman-Enskog gives accurate results in the case of the motion of molecules. Particles large compared to the mean free path of bath molecules can be described in the limit of the continuum approximation and the Stokes Einstein Debye equation gives the rotational friction in terms of macroscopic viscosity of medium. In the intermediate case of small particles approaching the molecule dimensions and in free molecular regimes various approximate solutions of transport equation have been proposed, from the Stokes-Cunningham to the generalized theory proposed by Lee and Wang [23, 24], which describe drag force under specular and diffusion scattering on the bases of kinetic theory. In particular, as particles approach molecule size, collisions with bath molecules can be described by specular scattering and the theory tend to the limit of Chapman-Enskog theory, conversely the limiting case of larger particles is described by diffusion scattering and tend to the Epstein model for hard sphere.
The drag coefficient k_d is therefore expressed as:

$$k_d = \xi m_p = \frac{8}{3}\sqrt{2\pi m_\gamma KT}\,NR^2\Omega_{avg}^{1.1*} \tag{7}$$

with $\Omega_{avg}^{1.1*}$ the average reduced collision integral, which has been reported in a parameterized form in ref. 24, m_r the reduced mass, N number concentration of bath molecules and R and m_p respectively the particle radius and mass.
The Langevin model is valid in the case of small angular steps and consequently for relatively high densities. A more appropriate description of the rotational motion of particles in a bath with low density is given by the J- and m- Diffusion model and J-coherence model developed by Gordon [25, 26].
These models describe the interaction with the bath molecules as discrete collisions, which randomize the direction of angular momentum J and follow the Poisson distribution. In the time interval between two collisions, τ_{coll}, the particles rotate as a free rotator, and arbitrarily large angular steps are possible. In m-diffusion model the magnitude of J remain constant while in j- diffusion model it is randomized over a thermal distribution at each collision. In this last model, the decay time of angular velocity autocorrelation function is not dependent on the solute-solvent interaction parameters since it is coincident to the time interval between two collisions, $\tau=\tau_{coll}$ which is determined by gas kinetic theory. This dependence is reintroduced by the J-coherence model in which at each collision j is distributed according to a function, which take accounts of interaction of solute with the solvent. $\Omega(t)$ result to be an exponential decaying function whose lifetime differ from τ_{coll} on dependence of the scrambling potency per collision of the solvent molecules. The proportionality constant

between t_ω and t_{coll} indicate the number of collision necessary to produce a de-correlation in the angular velocity of solute species [10].
These theories give a good description of the anisotropy. In a medium with sufficiently low friction, the coherent inertial motion of free rotor change little over the time for angular excursion of significant fraction of 2π, so anisotropy decreases from the initial value to a coherence dip which corresponds to the average rotor approximately perpendicular to the initial direction. The position of the dip depends by angular momentum distribution and the moment of inertia of rotor and is approximately $\tau_{rot}/4$. Then, anisotropy gradually approaches an asymptotic value by the virtue of the fact that under collisionless conditions the total angular momentum is conserved. This value is equal to 0.1 for a linear rotor and assumes different values for particles of different shapes. At higher pressures, the dip remains visible but the long time anisotropy decays to zero at a rate that increases with friction. At even more higher pressures, collisions reduce coherence in the motion, the dip is completely lost and anisotropy decays exponentially because of diffusive motion.

Experimental set up

A co-flowing laminar diffusion flame of ethylene was studied under atmospheric pressure conditions. The burner consists of a 12 mm diameter un-cooled vertical tube for the fuel and a concentric tube (108 mm i.d.) for air. Ethylene (3.85 cm^3/s) was commercially supplied with stated purity (99%). Filtered air (700 cm^3/s) was supplied from a laboratory compressor producing a non-smoking diffusion flame similar to the one studied in various previous studies [12-22].
The laser excitation source consisted of an amplified, Ti:Sa laser system, composed of a laser oscillator pumped by a solid-state laser and a Ti:Sa regenerative amplifier, pumped by another solid state Q-switched laser at a repetition rate of 1 kHz. The laser pulse length and energy were 100 fs and 0.4 mJ at λ = 780 nm. The radiation was then frequency-doubled to 385 nm by a (BBO) crystal. An half-wave plate and a Glan-laser UV polarizer provided a clean vertically polarized radiation. The fluorescence light was collected at 90°. In front of the detector, a second polarizer selected vertical or horizontal component of the fluorescence, and a high pass filter with cut off at 450 nm was used to collect the whole fluorescence emitted in the visible and reject scattering. A fast photomultiplier tube (PMT) connected to a 2 GHz band pass digital oscilloscope detected the fluorescence signals.
The instrument response function, fr(t), was nearly Gaussian, with a full width at half maximum τ_{rf} =0.6 ns [6-8] and the effective temporal profile of fluorescence was retrieved by a least squares iterative reconvolution. Flame temperature has been measured by a Pt/Pt-Rh thermocouple. The maximum temperature was around 1900 K on the edge of the flame and about 1200 K in the low temperature region in the central position.

Results

The parallel and orthogonal components of the fluorescence have been measured for various axial and radial positions in the flame. Typical results of the performed measurements are reported in Fig. 1.
The rise of orthogonal component of the fluorescence signal is delayed respect to the rise of parallel component because initially the emission momentum dipole has the same direction as the excitation beam and the orthogonal component appears because of the rotational motion of the fluorescent species. The rise time of the signals is strongly influenced by the instrumental rensponse time and the decay of the curve is only slightly slower than the rise showing that the fluorescence decays time is very fast, of the order of a nanosecond. The

difference in intensity of the two signal is indicative of the persistence of anisotropy for almost the total duration of both signals; in fact a complete depolarization of fluorescence signal is reached only about 4 ns after the initial rise of the signal.

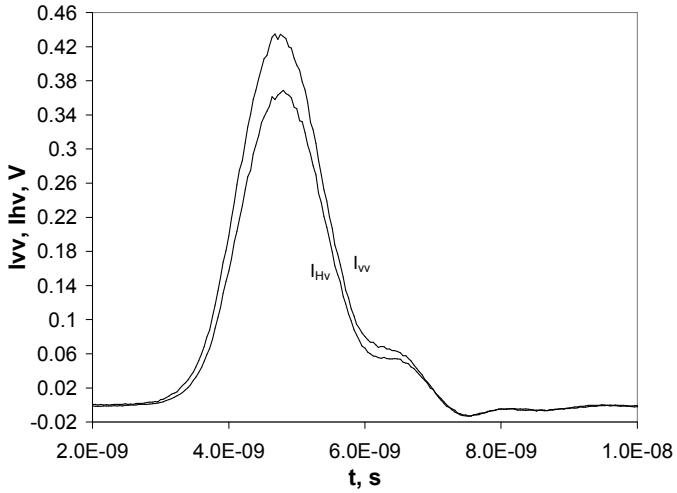

Figure 1. Parallel and orthogonal components of fluorescence, I_{VV} and I_{HV} measured at the height of 40 mm from the burner tip in the axial position.

From the measurements of I_{VV} and I_{HV} the intensity of fluorescence is given by $I_f=I_{VV}+2I_{HV}$. This quantity has been measured in various flame zones. The axial profile measured along the flame centerline and radial profiles measured at various flame heights are reported in Fig. 2 and 3.

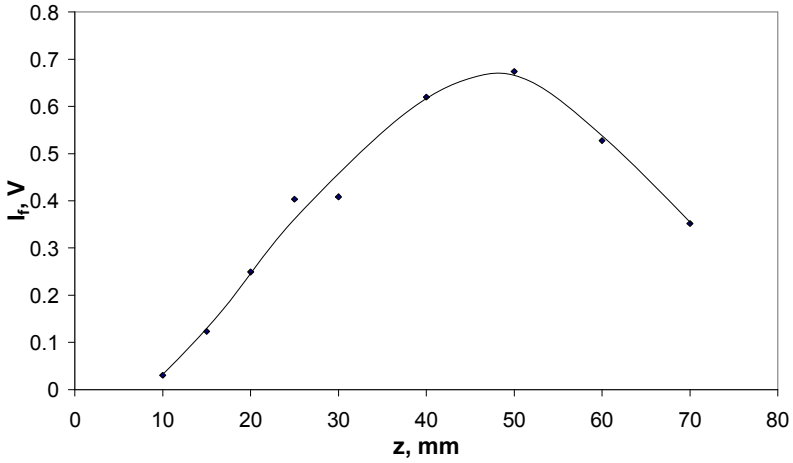

Figure 2. Axial profile of maximum fluorescence intensity measured along the flame centerline.

From the measurements of I_{VV} and I_{HV} the anisotropy, r(t), is determined according to equation (3).

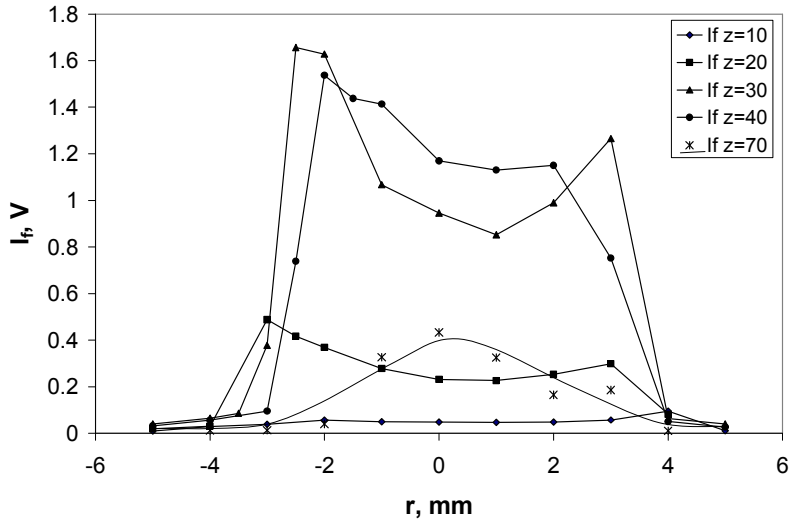

Figure 3. Radial profiles of maximum fluorescence intensity measured at various height above the burner.

In Fig. 4 the anisotropy obtained from data in Fig. 1 is reported. The value r0=0.4 is the theoretical value for the initial anisotropy when the absorption and emission dipole are parallel. In agreement to the Langevin model, the initial decrease is well approximated by a Gaussian curve and the further decrease by an exponential one.
At the flame conditions, T=1620 K, the decay time of angular velocity autocorrelation function, τ_ω, for particles with sizes from 1 to 10 nm is of the order of $1e^{-8}$ s. This is larger than the free rotational period τ_{free} and than the decay time of anisotropy, so that the dipole motion remains correlated. The correct theoretical model to describe anisotropy at flame condition is therefore the J coherence model. It predicts an initial fast decrease of a free rotor with a dip at ¼ period of rotation, followed by the realignment of the dipole and the final attainment of a constant limiting value that is due to the stationary distribution of angular momentum. The limiting r(t) contains therefore information on the shape of the fluorescing species, in fact. a value of roughly 0.1 is indicative of a linear shape of the fluorescing specie. A constant limiting value approximately constant was observed in the flame zones at lower temperature, future analysis will be performed to derive shape information from it. When collisions becomes more effective in scrambling the angular momentum the dip is gradually washed out and the dipoles monotonically tend to isotropy so that r(t) decays exponentially. This is the case reported in Fig. 4. Dashed lines indicate the Gaussian initial decay and the further exponential one.

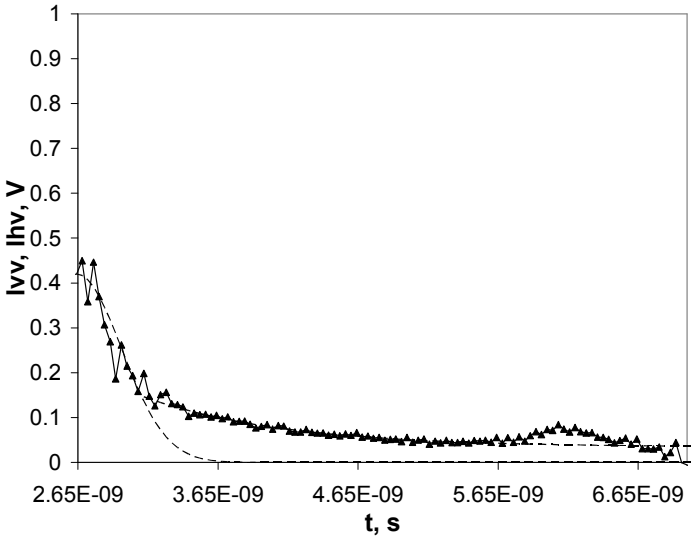

Figure 4. Anisotropy versus time obtained from data in Fig. 1. Data refers to the flame axis and at the height of 40 mm from the fuel nozzle.

According to eq. (6) the width of the Gaussian decay is equal to $w^2=I/6KT$; the latter is proportional to the particle momentum of inertia, I, and therefore depends on the particle size. For a spherical particle: $I=2/5m_pR^2$, so fitting the initial decay with a Gaussian curve it is possible to evaluate the particle radius given by:

$$R = \left(\frac{45}{4} \frac{KT}{\rho \pi} w^2 \right)^{1/5} \tag{8}$$

Since the Gaussian decay due to free rotation happen in a very fast time scale it is affected by large experimental uncertainties, a better estimate of the particle radius is given by the exponential decay.
According to eq. (5) in fact, the time constant of the exponential is $\tau_{rot}=1/(6D_r)$ with $D_r=KT/(\xi I)$ and the reduced friction constant ξ given by eq.(7). Since the decay time of the exponential is of the same order of magnitude as the instrumental response time, the actual decay was determined by a reconvolution procedure as done in a previous work [11].
The profiles of particle diameter obtained by these procedures are reported in Figs. 5 and 6.

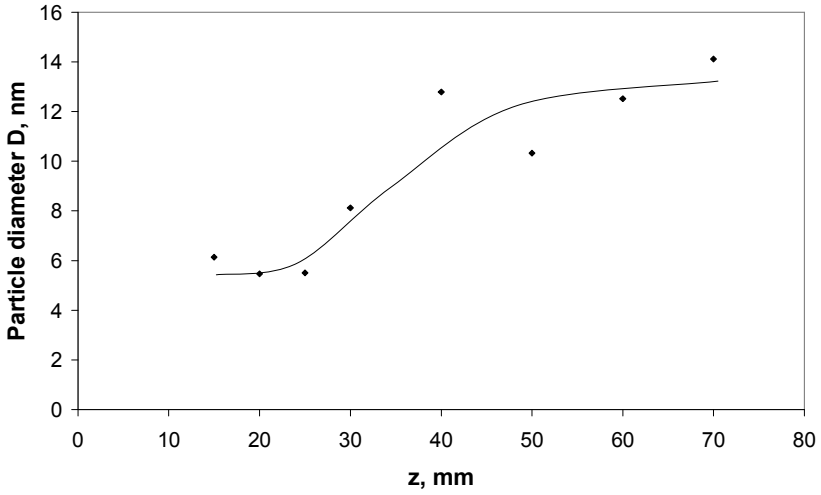

Figure 5. Profile of particle diameter versus the height above the burner measured on the flame centerline.

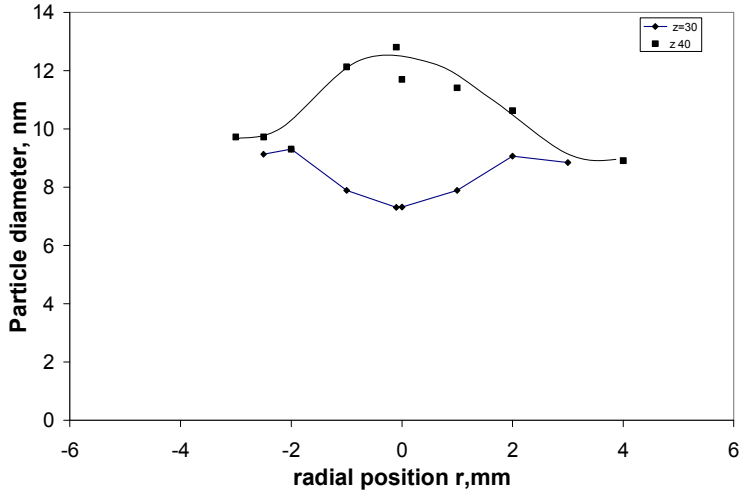

Figure 6. Radial profiles of particle diameter measured at two different heights above the burner.

Discussion

Flames similar to the one investigated in this work have been largely studied with a wide selection of experimental methods. This is a non smoking flame since particles are oxidized and do not exit the flame at its tip. According to data reported in the literature, we have observed that the amount of species which are excited by visible light and emit fluorescence in the visible strongly reduce high in the flame, above 50 mm, as evidenced by the relevant reduction of fluorescence intensity (Fig. 2). Comparing the radial profiles of Fig. 3 with the profiles of OH radical and soot measured by Santoro et al. [13], we observe that the maximum signal of visible fluorescing species is mainly detected in an anulus of the flame, internal to the flame front, and it extends towards the low temperature central zone of the flame, characterized by pyrolytic reactions. Soot particles, instead, have the maximum concentration in the inermediate region between the maximum of fluorescence and flame front [18-20].
Many works have investigated laser induced fluorescence in this flame. Measurements with excitation in the UV at 266 nm, performed by Vander Wal et al. [22], revealed the presence of

a so called “dark zone” intermediate between the PAH and soot zone where a relative lack of fluorescence and incandescence signal was observed. Furthermore, in the same study, and later by Megaridis and Dobbins [14-15], the use of Transmission Electron Microscopy (TEM) analysis revealed the presence of small particles of approximately 2-5 nm in size. So, the low laser induced emission was interpreted as due to species intermediate between a molecule and a solid particle that should not incandesce nor possess high fluorescence quantum efficiency. The results of the experiment here reported show that, in this flame zone, particles with sizes of about 5-20 nm that can be excited in the visible are present. From the time decay of fluorescence, signal the fluorescence lifetime result to be of the order of 1 ns. This is sensibly lower than the lifetime, reported by Vander Wal, of the fluorescence signals attributed to PAH, tens of nanoseconds, and it is consistent with a low quantum efficiency for these soot precursor particles with the fluorescence fastly quenched by internal conversion as hypothesized by Vander Wal. Incandescence signal is not detected by our experimental set up since the ultrafast excitation pulse, 100 fs, do not lasts enough time to heat up particles. All the measured signals are due to fluorescence and are not affected by interference from LII.
The laser induced fluorescence intensity is proportional to the volume fraction of fluorescing species with a proportionality factor which is dependent on the fluorescence cross section and quantum yield, so that in principle can vary sensibly along the flame. Nevertheless, it is interesting to compare fluorescence intensity profile of visible-selected particles, i.e. those species that absorb the radiation in the visible portion of the light spectrum and emit fluorescence in the visible, to the volume fraction of soot and Nanoparticles of Organic Carbon (NOC) determined in a previous paper [20] from light absorption in the visible and UV respectively. These radial profiles for the height of 20 mm are reported in fig. 7. It seems clear that the concentration of visible-selected particle has a trend intermediate between those of soot and NOC particles. In fact, the fluorescence intensity of visible-light-selected particles has the maximum value on the wings of the flame, slightly before the maximum of soot particles, and is still relevant in the central region, where NOC species have the maximum concentration and soot is absent.

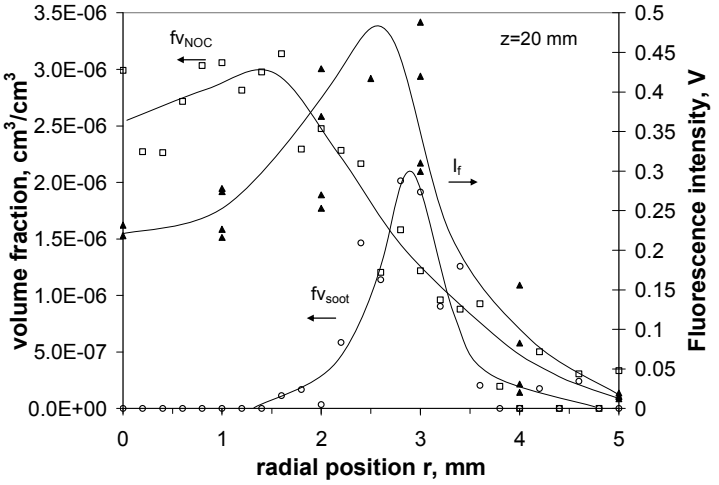

Figure 7. Radial profiles of fluorescence intensity measured at the heights above the burner of 20 mm compared to volume fraction of soot and NOC particles reported in ref. [20].

The analysis of fluorescence signals in terms of anisotropy has allowed to selectively determine the size of those particles chosen on the bases of their absorption and fluorescence properties. The visible-selected species have sizes between 5 to 15nm. Below z=30 nm the largest particles are found on the wings, near the flame zone where also the largest soot

particles are present [20], above this height the largest particles can be detected near the flame axis.

Conclusions

In this paper, the application of TRFA technique for the in situ analysis of nanometric particles in a diffusion flame has been presented.
We have used a femtosecond laser pulses in the visible as excitation source and a fast photomultiplier tube coupled with a digital oscilloscope with 2Ghz band-pass to detect fluorescence signal decay. A reconvolution method was used for data analysis. The experimental set-up achieves enough time resolution to detect particles in the size range between 5 and 30 nm.
We have studied a co-flowing laminar diffusion flame of ethylene under atmospheric pressure conditions. The flame is a non-smoking flame and was previously charachterized by a large variety of experimental methods [12-15, 17, 21, 22]. TRFA give average diameters of particles selected by their spectroscopic properties. The results obtained are in good agreement with previous analysis reported in literature and add useful information to complete the picture of particle formation in diffusion flame previously done in term of UV absorbing NOC particles and soot, by monitoring species with absorption and fluorescence bands extended in the visible wavelength region. These species have size of the order of 5-15 nm intermediate between those of NOC particles, of the order of 2-3 nm [20], and the mature soot.
The use of a laser source tunable from the deep UV to the visible for the TRFA analysis, would allow a complete characterization of soot precursors extending the analysis to the whole population of the fluorescing particles.

References

[1] D'Anna, A., Minutolo, A., "Combustion-formed nanoparticles", *Proc. Comb. Inst.* 32(1): 593-613 (2009).

[2] Oberdörster, G., Oberdörster, E., Oberdörster, J., "Nanotoxicology: an emerging discipline evolving from studies of ultrafine particles" *Environ. Health Perspect.* 113 (7): p. 823-839 (2005).

[3] Kennedy, Ian M., "The health effects of combustion-generated aerosols" *Proc. Combust. Inst.* 31 (2): 2757-2770 (2007).

[4] Karcher, B., "Aviation-produced aerosols and contrails" *Survey Geophys*. 20 (2): 113-167 (1999).

[5] Lakowicz, J.R., *Principles of Fluorescence Spectroscopy*, Plenum Press, 1983, p. 156.

[6] Bruno, A., de Lisio, C., Minutolo, P., "Time resolved fluorescence polarization anisotropy of carbonaceous particles produced in combustion systems" *Optics Express* 13 (14): p. 5393-5408 (2005).

[7] Bruno, A., Alfe, M., Apicella, B., de Lisio, C., Minutolo, P., "Characterization of nanometric carbon materials by time-resolved fluorescence polarization anisotropy" *Optics and Laser in Engineering* 44 (7): p. 732-746 (2006).

[8] Bruno, A., de Lisio, C., Minutolo, P., D'Alessio A., "Evidence of fluorescent carbon nanoparticles produced in premixed flames by time-resolved fluorescence polarization anisotropy" *Comb and Flame* 151: p. 472-481 (2007).

[9] Baskin, J. S., Gupta, M., Chachisvilis, M., Zewail, A. H., "Femtosecond dynamics of microscopic friction: nature of coherent versus diffusive motion from gas to liquid density" Chem. Phys. Lett. 275: 437-444 (1997).

[10] Baskin, J. S., Chachisvilis, M., Gupta, M., Zewail, A. H., "Femtosecond dynamics of solvation: microscopic friction and coherent motion in dense fluids" J. Phys. Chem. A 102: 4158-4171 (1998).
[11] Bruno, A., Ossler, F., de Lisio, C., Minutolo P., Spinelli N., D'Alessio A., "Detection of fluorescent nanoparticles in flame with femtosecond laser-induced fluorescence anisotropy" *Optics Express* 16 (8): p. 5623-5632 (2008).
[12] Santoro, R.J., Semerjian H.G., Dobbins, R.A., "Soot particle measurements in diffusion flames" *Combust. Flame* 51: p. 203–218 (1983).
[13] Santoro R.J., Yeh T.T., Howarth J.J., Semerjian, H.J., " The Transport and Growth of Soot Particles in Laminar Diffusion Flames" *Comb. Sci. Tech*. 53, 89-115 (1987).
[14] Megaridis C.M., Dobbins R.A., "Morphological Description of Flame-Generated Materials" *Comb. Sci. Tech.* 71 (1-3): p. 95-109 (1990).
[15] Megaridis C.M., Dobbins R.A., "Comparison of Soot Growth and Oxidation in Smoking and Non-Smoking Ethylene Diffusion Flames": *Comb. Sci. Tech.* 66 (1-3): p. 1-16 (1989).
[16] Kennedy, I.M., Yam, C., Rapp, D.C., Santoro R.J., "Modeling and measurements of soot and species in a laminar diffusion flame" *Comb and Flame* 107 (4): p. 368-382 (1996).
[17] McEnally, C.S., Koylu, U.O., Pfefferle, L.D., Dobbins R.A., "Soot volume fraction and temperature measurements in laminar nonpremixed flames using thermocouples" *Comb and Flame* 109 (4): p. 701-720 (1997).
[18] D'Anna, A., Kent, J.H., Santoro, R.J., "Investigation of species concentration and soot formation in a co-flowing diffusion flame of ethylene" *Comb. Sci. Tech.* 179 (1-2): 355-369 (2007).
[19] D'Anna, A., Kent, J.H., "Modeling of particulate carbon and species formation in coflowing diffusion flames of ethylene" *Comb and Flame* 144 (1-2): 249-260 (2006).
[20] D'Anna, A., Rolando, A., Allouis, C., Minutolo P., D'Alessio A., "Nano-organic carbon and soot particle measurements in a laminar ethylene diffusion flame" *Proc. Combust. Inst.* 30: 1449-1456 (2005).
[21] Vander Wal, R.L., "Soot precursor carbonization: Visualization using LIF and LII and comparison using bright and dark field TEM" *Comb and Flame* 112 (4): p. 607-616 (1998).
[22] Vander Wal, R.L., Jensen, K.A., Choi, M. Y., "Simultaneous laser-induced emission of soot and polycyclic aromatic hydrocarbons within a gas jet diffusion flame" *Comb and Flame* 109: p. 399-414 (1997).
[23] Li, Z.G., Wang, H., "Drag Force, Diffusion Coefficient, and Electric Mobility of Small Particles. I. Theory Applicable to the Free-molecule Regime" *Phys. Rev. E.* 68(6): 061206-1 - 061206-9 (2003).
[24] Li, Z.G., Wang, H., "Drag Force, Diffusion Coefficient, and Electric Mobility of Small particles. II. Application" *Phys. Rev. E.* 68(6): 061207-1 - 061207-13 (2003).
[25] Gordon, R. G., "Molecular motion in infrared and Raman spectra" J. Chem. Phys. 43: 1307-1312 (1965).
[26] Gordon, R. G., "On the rotational diffusion of molecules" J. Chem. Phys. 44: 1830-1836 (1966).